Published in *Nature* **389**, 463-466 (1997).

Analogue experiments on irreversibility of classical fluctuations

D.G. Luchinsky*† and P.V.E. McClintock*

*School of Physics and Chemistry, Lancaster University, Lancaster, LA1 4YB, UK.

†Permanent address: Russian Research Institute for Metrological Service, Ozernaya 46, 119361 Moscow, Russia.

LARGE FLUCTUATIONS occur universally in Nature. They are responsible for e.g. nucleation at phase transitions, chemical reactions, mutations in DNA sequences, protein transport in biological cells, and failures of electronic devices. The idea[1,2] that they provide a conceptual bridge between microscopic and macroscopic motion underlies many discussions[2–5] of how the irreversible thermodynamic behaviour of matter in bulk relates to the completely reversible (classical or quantum) mechanical laws describing its constituent atoms or molecules. The theory of large fluctuations has been developed through e.g. Hamiltonian[6,7] and equivalent path-integral[8–12] formulations. It remains largely untested, partly on account of the rarity of such events, and partly because the possibility of quantitative experiments could not be entertained until the appropriate statistical quantity (prehistory probability distribution[11]) had been introduced. Recent analogue electronic experiments have shown[12], however, that there are physically observable patterns of trajectories underlying the seemingly random motion. In what follows, we extend the experimental technique to highlight a fundamental distinction between *fluctuational motion* towards the remote state and ordinary *relaxational motion* back again towards the stable state of the system.

In a typical large fluctuation, a component x of some dynamical variable $\mathbf{x}$ departs temporarily from its stable state, moves to a remote state x_f, and then returns: see e.g. Fig. 1(a). The variable $\mathbf{x}$ might represent the voltage(s) in an electrical circuit (see below), or the phase of the order parameter in a SQUID (superconducting quantum interference device)[13] or in an optical bistable device[14], or the number densities of species in a chemical reaction[15]. Approximate theories of such phenomena have been developed[6,7,9–12,15–21], the

approach being typically as follows. Consider overdamped Brownian motion in a force field $\mathbf{K}(\mathbf{x},t)$, assumed in general to be nonadiabatic and/or nongradient, driven by weak white noise $\xi(t)$ whose intensity $D \ll 1$ is considered to be the smallest parameter of the problem

$$\dot{\mathbf{x}} = \mathbf{K}(\mathbf{x},t) + \xi(t), \tag{1}$$

$$\langle \xi(t) \rangle = 0, \quad \langle \xi(t)\xi(0) \rangle = D\delta(t).$$

The corresponding Fokker-Plank equation (FPE) for the probability density $P(\mathbf{x},t)$ is

$$\frac{\partial P(\mathbf{x},t)}{\partial t} = -\nabla \cdot (\mathbf{K}(\mathbf{x},t)\, P(\mathbf{x},t)) + \frac{D}{2}\nabla^2 P(\mathbf{x},t). \tag{2}$$

A large fluctuation is Brownian motion away from a stable stationary state S. It is similar to quantum mechanical tunnelling through a potential barrier, and can be treated in a similar way. In the limit of weak noise it can be described by the WKB (eikonal) approximation of the FPE in the form $P(\mathbf{x},t) = z(\mathbf{x},t)\exp\left(-\frac{W(\mathbf{x},t)}{D}\right)$. Here $z(\mathbf{x},t)$ is a prefactor, and $W(\mathbf{x},t)$ is a classical action satisfying the Hamilton-Jacobi equation, which can be solved by integrating the Hamiltonian equations of motion[7]

$$\dot{\mathbf{x}} = \mathbf{p} + \mathbf{K}, \quad \dot{\mathbf{p}} = -\frac{\partial \mathbf{K}}{\partial \mathbf{x}}\mathbf{p}, \tag{3}$$

$$H(\mathbf{x},\mathbf{p},t) = \mathbf{p}\,\mathbf{K}(\mathbf{x},t) + \frac{1}{2}\mathbf{p}^2, \quad \mathbf{p} \equiv \nabla W,$$

We emphasise that (3) describe an *auxiliary* Hamiltonian system which should be carefully distinguished from the microscopic Hamiltonian equations of motion in a thermal system. Note also that the method is readily generalised, e.g. to systems driven by coloured noise[10,20,21].

The set of trajectories of (3) approaching the stable state S ($\bar{x} = x_s, \bar{\mathbf{p}} = 0$) for positive time forms the stable invariant manifold of S, defined by the additional condition $\mathbf{p} = \mathbf{0}$. On this manifold, (3) reduces to $\dot{\mathbf{x}} = \mathbf{K}$, describing deterministic relaxation, so that these trajectories must correspond to the return path of the initial system (1) from x_f to S. The set of trajectories moving away from S in positive time forms the unstable invariant manifold of S, upon which $\mathbf{p} \neq \mathbf{0}$ in (3); they can be identified as describing the fluctuational paths from S to x_f. In each case, the trajectories represent[6,7] optimal paths

along which the system is expected to move with overwhelming probability during the fluctuation. But, although the decay of the fluctuation was well understood[22], it remained uncertain for a long time whether or how the growth of a fluctuation along a trajectory of the unstable manifold might be observed experimentally. One problem was that noise in real systems is always of finite intensity, so that the relevance of the $D \to 0$ theory, for which the probability of having a large fluctuation at all also $\to 0$, was unclear. An additional puzzle originated in the analogy with optics and quantum mechanics[23] which, supplemented by a large body of numerical results, suggested[15,18–21,24–26] that patterns of optimal fluctuational paths in general display singular features, but ones that differ significantly[18,24,25] from those familiar from optics. It was sometimes inferred that the approximations leading to (3) would fail near the singularity points where, instead, a complete solution of the FPE (2) would be required[27].

More recently, however, the physical reality both of the paths, and of the singular features in their pattern, have been demonstrated[11,12] in analogue electronic experiments. Note that, if the (approximate) Hamiltonian description is correct, similar behavour is to be expected of *any* fluctuating system describable in terms of (1); analogue electronic circuits are especially advantageous for such studies because their parameters are well controlled. The technique[11,28] involves building an electronic circuit to model the system of interest, and driving it with external noise. Provided that no additional forces are applied, the system can be considered to be in thermal equilibrium at a temperature determined by the noise intensity and the damping constant, which are linked by the fluctuation dissipation theorem[3]. The state of the system is monitored continuously until eventually, as shown in Fig. 1(a), a large fluctuation reaches the voltage x_f. The interesting region of the path – including the fluctuational part f coming to x_f, as well as the relaxational part r leading back towards S – is then stored. An ensemble-average of such trajectories (Fig. 1(b)), built up over a period of time (typically weeks), creates the distribution $P_f(x,t) \equiv P(x_i,t_i;x,t;x_f,t_f)$, the probability of the system being at x at time t if it was at x_f at time t_f, with $t_f = 0$ and $x_i = x_s$ at time $t_i = -\infty$. Unlike the original definition[11] of the prehistory distribution, $t > t_f$ is considered as well as $t < t_f$.

We now consider the application of these ideas to the fluctuations of three very different example systems that can be used to describe a wide range of physical phenomena[13–15,22,27,29]. The first (Fig. 1) is an overdamped Duffing oscillator, modelling a bistable system in ther-

mal equilibrium near one of its stable states. Fig. 1(b) shows a meaured $P_f(x,t)$. It was found: (i) that the relaxational and fluctuational parts of the distribution are symmetrical, which would only be expected[4] under conditions of detailed balance (i.e. when every transition between two states in one direction is on average balanced by a transition in the opposite direction); (ii) that the ridges (modes) of the distribution follow closely the deterministic trajectory found from (3), plotted as the full curve in Fig. 1(c); and hence (iii) that, in the macroscopic limit, where the width of the distribution tends to zero (because $D \to 0$) and one observes only the positions of the ridges, the paths to/from x_f themselves become reversible in time[7,15,21,26]. Even in thermal equilibrium, however, Hamiltonian theory envisages the fluctuational and relaxational trajectories as belonging to two different manifolds of the system (3), with $\mathbf{p} \neq 0$ and $\mathbf{p} = 0$ respectively (see above). In the particular case of our analogue electronic model, this feature can be illustrated experimentally because the noise is external and a direct determination of p during fluctuations is therefore possible (c.f. the idea[8–10,20] of the *optimal force*). Thus we have been able to make simultaneous measurements of $x(t)$ and of the corresponding noise histories $\xi(t)$ causing transitions between the potential wells, setting $x_f = 0$ on the local potential maximum: some results are shown in Fig. 1(d). Although the statistics of these very rare events are relatively poor, the data clearly demonstrate: (i) that, as anticipated, $p \neq 0$ during the fluctuational part of the trajectory; (ii) that $p = 0$ within experimental error during relaxation; and (iii) that the Hamiltonian theory (curves) describes very well both parts of the trajectory. Thus the time reversal symmetry can be regarded as arising from a degeneracy between the projections of two different curves in an extended (by the **p**-dimension(s)) phase space onto the space of the dynamical variables. Such an extension of the phase space is an unnecessary complication in equilibrium; but it provides the key to understanding far-from-equilibrium systems, where the degeneracy is lifted by the presence of an external field.

Our second example (Fig. 2), is the archetypal nonequilibrium system considered by Graham[16,17] in his discussion of the properties of the generalised potential, and further analysed in great detail by Dykman and Smelyanskiy (to be published): an overdamped Duffing oscillator driven from equilibrium by a periodic force. The ridges of the fluctuational and relaxational parts of the measured $P_f(x,t)$ are narrow and differ markedly in

shape. The paths that they trace out (data points), compared in Fig 2(a) with theoretical predictions (curves) calculated from (3), clearly demonstrate that the most probable fluctuational trajectory to (x_f, t_f) does *not* correspond to what one would obtain by time-reversing the relaxational trajectory. Fig. 2(b) shows the measured $P_f(x,t)$ when x_f is placed on the calculated *switching line*[18], a singularity separating regions that are approached via different fluctuational paths. The relaxational tail leading back to the stable state S is common to the two fluctuational paths that form the resultant corral[12]. From Fig. 2(c) we see that the ridges of the distribution are strongly asymmetric in time, but agree well with the fluctuational and relaxational paths predicted from (3). The observed asymmetry of the distribution implies[4] a lack of detailed balance; and it leads directly[15,26] to macroscopic irreversibility in the $D \to 0$ limit where the width of the distribution tends to zero. In verifying the existence of the switching line, the results demonstrate the nondifferentiability of the generalised nonequilibrium potential.

Our third example (Fig. 3) is the system suggested by Maier and Stein[19,26] for analysis of the escape problem in nonequilibrium systems. It consists of a bistable system driven from equilibrium by a stationary field of (in general) the nongradient type. In measurements near one of the stable states, the lack of detailed balance and the irreversibility of the fluctuations become strikingly apparent. Fig. 3(a) shows the measured $P_f(x,y)$ distribution for fluctuations to the two different remote states $\mathbf{x_f}$ placed symmetrically on either side of the y axis; $P_f(x,y)$ is the projection of $P_f(x_i, y_i, t_i; x, y, t; x_f, y_f, t_f)$ onto the $x-y$ plane with $t_f = 0$ as before. When the paths traced out by the ridges are plotted (Fig. 3(b)), it can be seen: (i) that the fluctuational trajectories are completely different from the relaxational ones; and (ii) that they are in good agreement with the fluctuational and relaxational trajectories predicted from (3). Fig. 3(c) shows the corresponding picture measured for fluctuations to a *single* remote state $\mathbf{x_f}$ on the switching line (lying on the x axis). The two fluctuational paths to the remote state are, again, markedly different from the common relaxational path leading back to S. Both parts of the trajectory are well described by the corresponding optimal paths calculated from (3). In this case too, therefore, the observations link a lack of detailed balance to macroscopic irreversibility, and demonstrate the nondifferentiability of the generalised nonequilibrium potential; the closed loops traversed during fluctuations verify the expected[2,26,27] occur-

rence of rotational flow in nonequilibrium systems.

Thus, after more than 60 years of "thought experiments" on large fluctuations[2,3,30], it has now become possible to do real ones, yielding quantitative results. The work has already verified several long-standing theoretical predictions, including those of symmetry between the growth and decay of classical fluctuations in equilibrium[2,30], the breaking of this symmetry under nonequilibrium conditions[7,15,26], the relationship of symmetry-breaking to a lack of detailed balance[15–17,26] and to nondifferentiability of the generalised nonequilibrium potential[16,17,26], and the existence of an optimal force derived from the fluctuating field and related to the momentum of an auxiliary Hamiltonian system[8–10,20,21]. The technique has also enabled us to reveal new dynamical features of large fluctuations, such as critical broadening of the prehistory probability distribution[12]. It will be as applicable to future experiments on natural systems as it has been to the electronic models studied here. Because equations (1) can, at least in some cases[9,31], be related directly to the microscopic classical equations of motion for a system interacting with a heat bath, the approach illuminates connections between microscopic reversibility and macroscopic irreversibility. Other open questions needing urgently to be addressed include the precise physical meaning of the momentum **p** and the role of entropy and how it changes during fluctuational motion.

References

1. Einstein, A. Investigations on the theory of the Brownian movement. *Ann. d. Phys* **17**, 549 (1905) and associated papers reprinted in translation in *Investigations on the theory of the Brownian movement*, ed. R. Fürth (Dover, New York, 1956).

2. Onsager, L. Reciprocal relations in irreversible processes. I. *Phys. Rev.* **37**, 405-426 (1931).

3. L.D. Landau and E.M. Lifshitz, *Statistical Physics*, 3rd ed., Part 1 (Pergamon, New York 1980).

4. Schulman, L.S. Models for intermediate time dynamics with two-time boundary conditions. *Physica A* **117**, 373-380 (1991).

5. Bricmont, J. Science of chaos or chaos in science? *Ann. New York Acad. Sci.* **775**, 131-175 (1996).

6. Cohen, J.K. and Lewis, R.M. A ray method for the asymptotic solution of the diffusion equation. *J. Inst. Math. Appl.* **3**, 266-290 (1967).

7. Freidlin, M.I. and Wentzell, A.D. *Random Perturbations in Dynamical Systems* (Springer-Verlag, New York, 1984).

8. Feynman, R.P. and Hibbs, A.R. *Quantum Mechanics and Path Integrals* (McGraw-Hill, New York, 1965).

9. Dykman, M.I. and Krivoglaz, M.A. Theory of nonlinear oscillator interacting with medium. In *Soviet Physics Reviews*, ed. Khalatnikov, I.M. (Harwood, New York, 1984), vol. 5, pp. 265-441.

10. Bray, A.J. and McKane, A.J. Instanton calculation of the escape rate for activation over a potential barrier driven by colored noise. *Phys. Rev. Lett.* **62**, 493-496 (1989).

11. Dykman, M.I., McClintock, P.V.E., Smelyanskiy, V.N., Stein, N.D. and Stocks, N.G. Optimal paths and the prehistory problem for large fluctuations in noise-driven systems. *Phys. Rev. Lett.* **68**, 2718-2721 (1992).

12. Dykman, M.I., Luchinsky, D.G., McClintock, P.V.E. and Smelyanskiy, V.N. Corrals and critical behaviour of the distribution of optimal paths. *Phys. Rev. Lett.* **77**, 5229-5232 (1996).

13. Kautz, R.L. Noise, chaos, and the Josephson standard. *Rep. Prog. Phys.* **59**, 935-992 (1996).

14. Dykman M.I., Golubev G.P., Kaufman I.Kh., Luchinsky D.G., McClintock P.V.E., and Zhukov E.A. Noise-enhanced optical heterodyning. *Appl. Phys. Lett.* **67**, 308-310 (1995).

15. Dykman, M.I., Mori, E., Ross, J. and Hunt, P.M. Large fluctuations and optimal paths in chemical kinetics. *J. Chem. Phys.* **100**, 5735-5750 (1994).

16. Graham, R. and Tél, T. Existence of a potential for dissipative dynamical systems. *Phys. Rev. Lett.* **52**, 9-12 (1984).

17. Graham, R. Macroscopic potentials, bifurcations and noise in dissipative systems. In *Noise in Nonlinear Dynamical Systems*, ed. F. Moss and P. V. E. McClintock (Cambridge University Press, 1989), vol. 1, pp 225-278.

18. Dykman, M.I., Millonas, M.M. and Smelyanskiy, V.N. Observable and hidden features of large fluctuations in nonequilibrium systems. *Phys. Lett. A* **195** 53-58 (1994).

19. Maier, R.S. and Stein, D.L. A scaling theory of bifurcations in the symmetrical weak-noise escape problem. *J. Stat. Phys.* **83**, 291-357 (1996).

20. Dykman, M.I. Large fluctuations and fluctuational transitions in systems driven by colored Gaussian noise – a high-frequency noise. *Phys. Rev. A* **42**, 2020-2029 (1990).

21. Einchcomb, S.J.B. and McKane, A.J. Use of Hamiltonian mechanics in systems driven by colored noise. *Phys. Rev. E* **51**, 2974-2981 (1995).

22. Van Kampen, N.G. *Stochastic Processes in Physics and Chemistry* (Elsevier, Amsterdam, 1990).

23. Berry, M.V. Waves and Thom's theorem. *Adv. Phys.* **25**, 1-26 (1976).

24. Jauslin, H.R. Nondifferentiable potentials for nonequilibrium steady states. *Physica A* **144**, 179-191 (1987).

25. Day, M.V. Recent progress on the small parameter exit problem. *Stochastics* **20**, 121-150 (1987).

26. Maier, R.S. and Stein, D.L. Escape problem for irreversible systems. *Phys. Rev. E* **48**, 931-938 (1993).

27. Risken, H. *The Fokker-Planck Equation*, 2nd ed. (Springer, Berlin, 1989).

28. McClintock, P.V.E. and Moss, F. Analogue techniques for the study of problems in stochastic nonlinear dynamics. In *Noise in Nonlinear Dynamical Systems*, ed. F. Moss and P. V. E. McClintock (Cambridge University Press, 1989), vol. 3, pp 243-274.

29. Haken, H. Cooperative phenomena in systems far from thermal equilibrium and in nonphysical systems. *Rev. Mod. Phys.* **47** 67-119 (1975).

30. Onsager, L. and Machlup, S. Fluctuations and irreversible processes. *Phys. Rev.* **91**, 1505-1512 (1953).

31. Zwanzig, R. Nonlinear generalised Langevin equations. *J. Stat. Phys.* **9**, 215-220 (1973).

ACKNOWLEDGEMENTS The research, supported by the Engineering and Physical Sciences Research Council (UK), the Royal Society of London, and the Russian Foundation for Basic Research could not have been attempted without the continuing help and encouragement of M I Dykman. We are indebted to him and to D L Stein for valuable comments on an earlier version of the manuscript.

Figure Captions

1. Fluctuational behaviour measured and calculated for an electronic model system in equilibrium: a double-well Duffing oscillator with $K(x) = x - x^3$, for $D = 0.014$. The model was constructed[28] from standard electronic components (e.g. operational amplifiers and analogue multipliers), tested for accuracy, and then treated as an entity in its own right – an object on which experiments could be performed. It was driven by external noise (a fluctuating voltage) from a noise generator, causing it to fluctuate about its equilibrium state at -1.0 volts, representing $\bar{x} = x_s = -1$ in (1). This response, a fluctuating voltage representing $x(t)$, was then digitised and analysed with a digital data processor. In particular, $x(t)$ was monitored continuously, waiting for large fluctuations reaching a chosen preset voltage threshold representing x_f. Fluctuational paths $x(t)$ reaching x_f were preserved for later analysis, and so also were the relaxational paths $x(t)$ from x_f back towards the stable state at $x = -1$. (a) Two typical fluctuations (jagged lines) from the stable state at $S = -1$ to the remote state $x_f = -0.1$, and back again, are compared with the deterministic (noise-free) relaxational path from x_f to S (full, smooth, curve) and its time-reversed ($t \to -t$) mirror image (dashed curve). The fluctuational and relaxational parts of the trajectory are labelled f and r respectively. (b) The probability distribution $P_f(x,t)$ built up by ensemble-averaging a sequence of trajectories like those in (a). The top-plane plots the positions of the ridges of $P_f(x,t)$ for the fluctuational (open circles) and relaxational (asterisks) parts of the trajectory for comparison with theoretical predictions (curves) based on (3). (c) Plots of the ridges of $P_f(x,t)$, with $t \to -t$ for the relaxational part, demonstrating the time-reversal symmetry. The full curve is the theoretical prediction based on (3). Inset: detailed balance means that, for every transition in one direction between any two levels (e.g. those shown by the dashed lines), there must be a return transition in the opposite direction, i.e. given that a relaxational trajectory exists, the corresponding fluctuational one must be its time-inversed image in configuration space, so that detailed balance implies time-reversal symmetry. (d) Demonstration of time-*irreversible* features of the fluctuations. The inset shows $p(x)$ for two typical transitional paths from $x = -1$ to $x = 1$ (full jagged line) and in the opposite direction (dotted jagged line). The main

figure shows the paths traced out by the ridges of the $P_f(p,x)$ distribution created from an ensemble average of such transitions. The transitional path from $x=-1$ to $x=1$ is shown by squares, and the reverse transition by filled circles. The full and dashed curves are the corresponding paths predicted from (3).

2. Fluctuational behaviour measured and calculated for an electronic model of a nonequilibrium system with explicit time dependence: an overdamped double-well Duffing oscillator with $K(x,t)=x-x^3+A\cos(\omega t)$ and $A=0.264$, $D=0.012$. (a) Fluctuational and relaxational paths (red circles and blue asterisks respectively) to/from the remote state $x_f=-0.46, t=0.73$, found by tracing the ridges of a measured $P_f(x,t)$ distribution. The time-dependent stable and unstable states near $x=-1$ and $x=0$ are shown by dashed lines. The fluctuational and relaxational paths calculated from (3) are shown as red and blue lines respectively. (b) The measured $P_f(x,t)$ for a remote state $x_f=-0.63$, $t=0.83$ that lies on the switching line. (c) Fluctuational (red circles) and relaxational (blue asterisks) paths determined by tracing the ridges of the distribution in (b), and compared with the corresponding (red and blue) theoretical lines predicted from (3).

3. Fluctuational behaviour measured and calculated for an electronic model of a nonequilibrium system with a stationary nongradient field:
$\mathbf{K}(x,y)=(x-x^3-axy^2,-(1+x^2)y)$; $a=10$; $D=0.014$. (a) The $P_f(x,y)$ distribution created by ensemble-averaging fluctuational paths leading from $S=(1,0)$ to remote points at $\mathbf{x_f}=(0.44,\pm 0.35)$. (b) Paths traced out by the ridges of the distribution in (a) for fluctuational motion (red circles), and by those of the corresponding distribution for relaxational motion (blue asterisks), compared with fluctuational (red) and relaxational (blue) optimal paths calculated from (3). (c) As in (b), but for the *single* remote state $\mathbf{x_f}=(0.32,0)$ on the switching line.

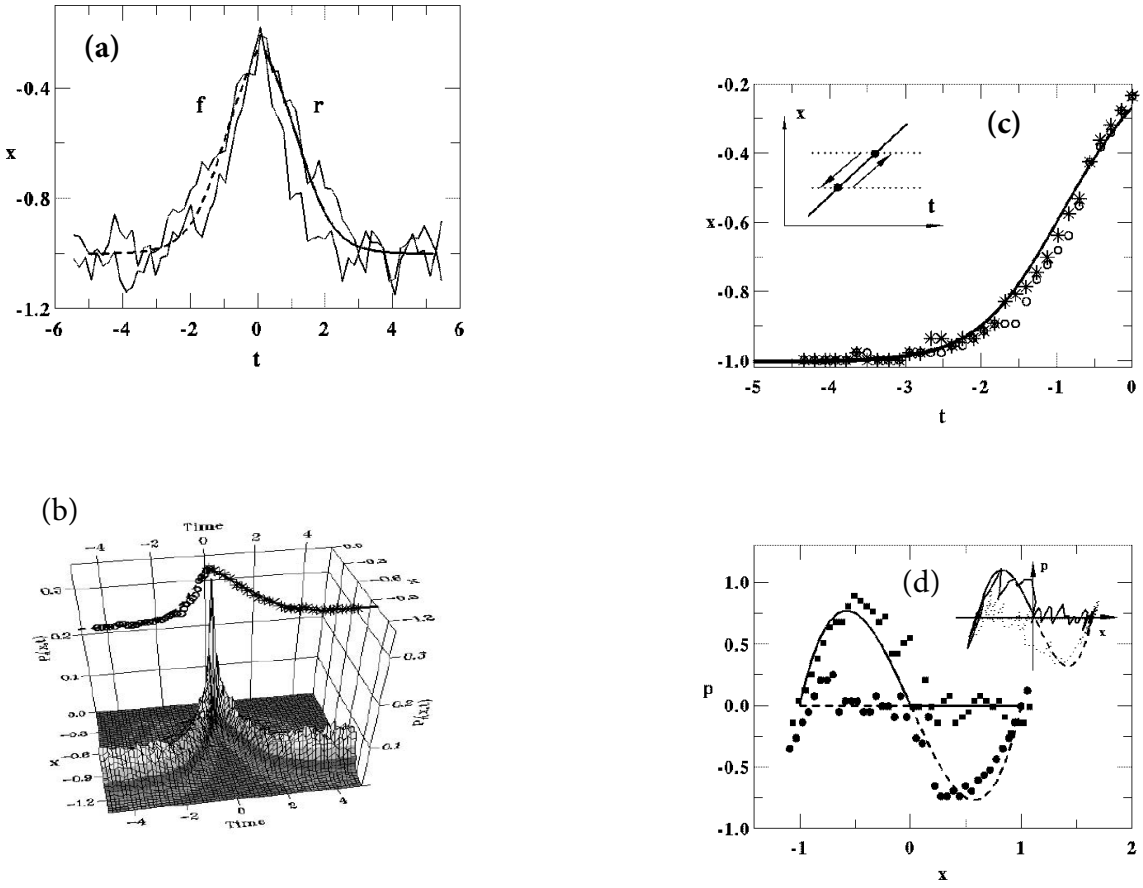

Figure 1:

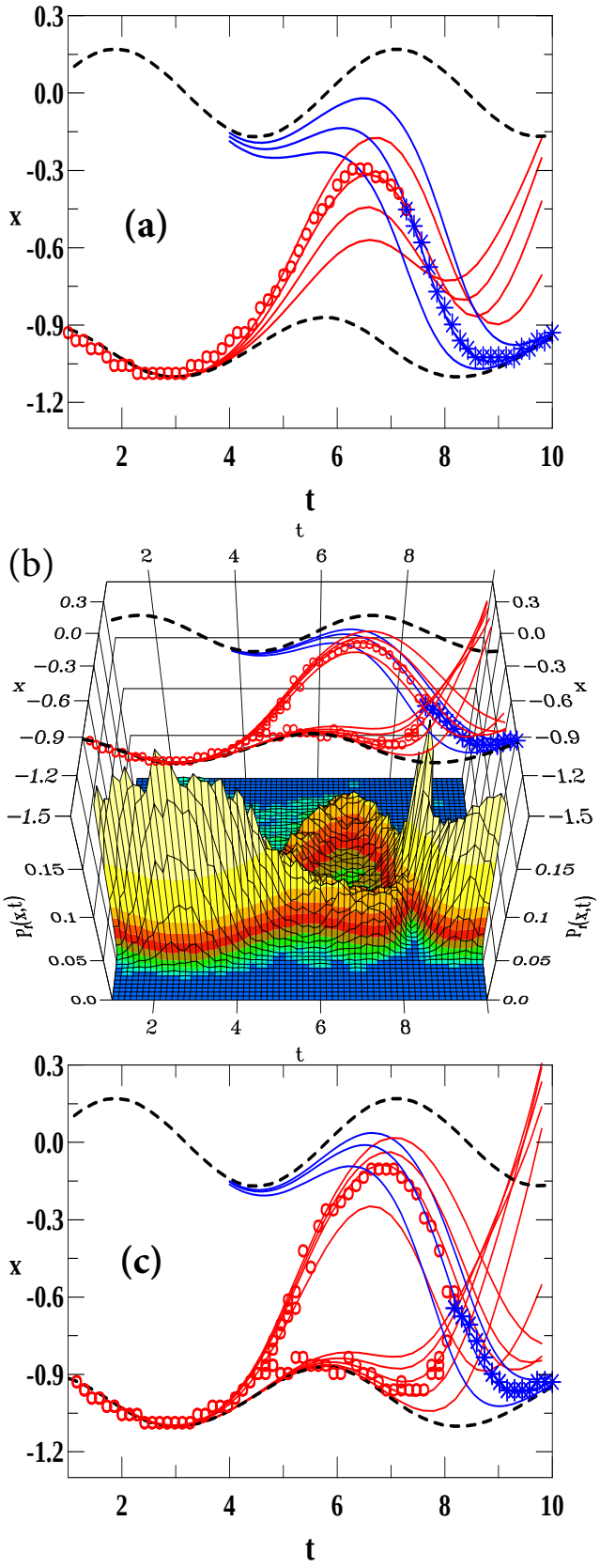

Figure 2:

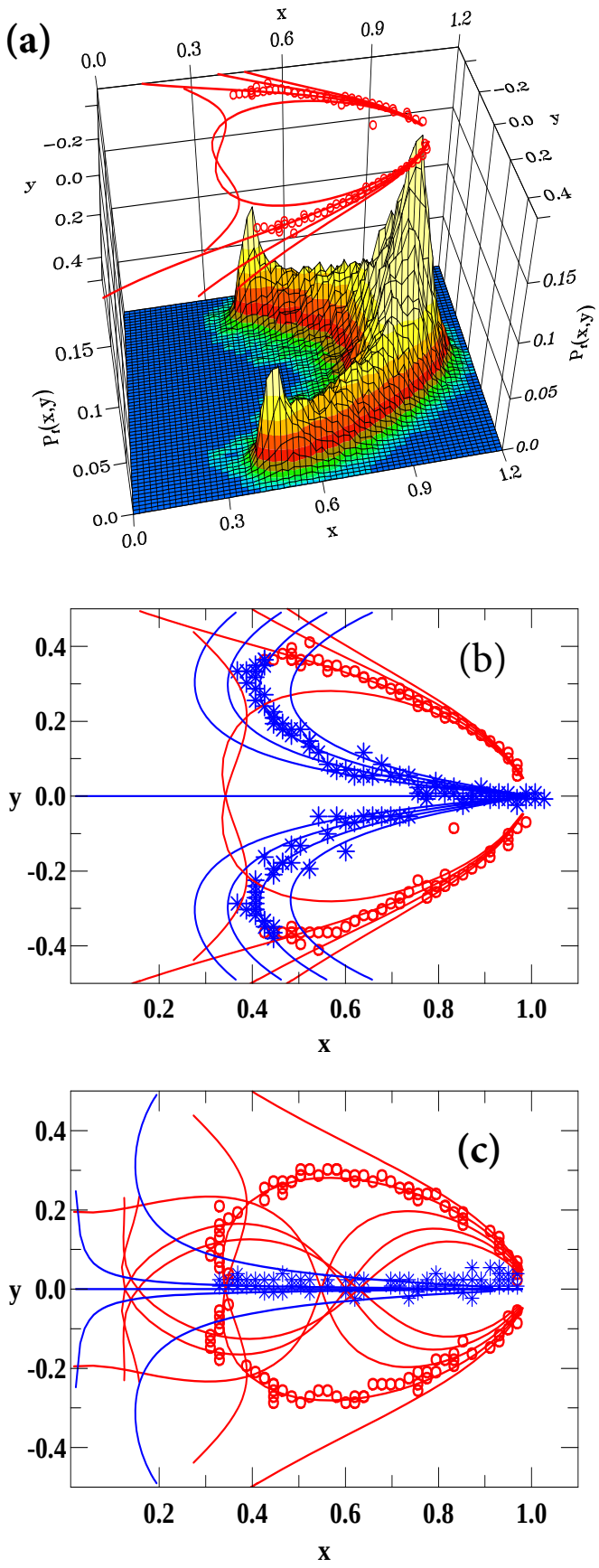
(a)
x
0.0
0.3
0.6
0.9
1.2
y
−0.2
0.0
0.2
0.4
P_t(x,y)
0.15
0.1
0.05
0.0
(b)
(c)
0.4
0.2
y 0.0
-0.2
-0.4
0.2
0.4
0.6
0.8
1.0
x

Figure 3: